

# Overexpression of the human 2-oxoglutarate carrier lowers mitochondrial membrane potential in HEK-293 cells: contrast with the unique cold-induced mitochondrial carrier CGI-69

Xing Xian YU\*, David A. LEWIN†, Alan ZHONG‡, Jennifer BRUSH‡, Peter W. SCHOW§, Steven W. SHERWOOD§, Guohua PAN\* and Sean H. ADAMS\*<sup>1</sup>

\*Department of Endocrinology, Genentech, Inc., 1 DNA Way, South San Francisco, CA 94080, U.S.A., †Department of Gene Discovery, CuraGen Corporation, New Haven, CT 06511, U.S.A., ‡Department of Molecular Biology, Genentech, Inc., 1 DNA Way, South San Francisco, CA 94080, U.S.A., and §Department of Bioassay and Bioluminescence, Genentech, Inc., 1 DNA Way, South San Francisco, CA 94080, U.S.A.

Using differential mRNA expression analysis, a previously uncharacterized gene was found to be up-regulated 2-fold in brown adipose tissue (BAT) of mice exposed to cold (4 °C) for 48 h. Contig and homology analysis revealed that the gene represents the murine orthologue to a sequence from a public database encoding a putative human protein (CGI-69). The presence of mitochondrial carrier domains in the human protein, its transmembrane topology and cold-induction of the mouse CGI-69 gene in BAT prompted an analysis of the idea that CGI-69 may represent a new uncoupling protein (UCP) functional homologue. However, transfection of human CGI-69 isoforms in

HEK-293 cells yielded no change in mitochondrial membrane potential ( $\Delta\psi_m$ ), despite localization of FLAG-tagged CGI-69 to mitochondria of MCF7 cells. Surprisingly, overexpression of the human 2-oxoglutarate carrier (OGC) protein (originally designed as a negative control) sparked a significant drop in  $\Delta\psi_m$ , possibly signalling a previously unappreciated uncoupling activity for the OGC.

**Key words:** metabolic rate, oxidative phosphorylation, reactive oxygen species, respiration, thermogenesis.

## INTRODUCTION

The bulk of animal-tissue oxygen consumption is driven by a finely balanced system in which the rate of mitochondrial catabolism of fuels is regulated largely by the flow of electrons along the electron-transport chain. Concomitant pumping of protons outwards across the mitochondrial inner membrane establishes a proton electrochemical gradient or protonmotive force ( $\Delta p$ ), which drives ATP synthesis via inward flow of protons through  $F_1F_0$ -ATP synthase. Thus fuel combustion, electron transport, proton flux and ATP turnover are intimately coupled. However, a portion of the  $\Delta p$  is dissipated as protons flow inwards independently of ATP synthase, a phenomenon termed proton leak or uncoupling. Fuel combustion and electron transport/outward proton pumping increase in response to dissipation of  $\Delta p$ ; thus, innate mitochondrial proton leak may account for a significant amount of daily energy expenditure (estimated to be 20–40 % of tissue metabolic rate) [1,2]. Clarifying the molecular basis of proton leak is an active area of research, and holds promise in uncovering target pathways for pharmaceutical intervention to treat obesity and other diseases arising from perturbations of energy balance.

The first clue that specific proteins may underlie mammalian mitochondrial proton leak emerged from studies of brown adipose tissue (BAT), a specialized tissue in which a large proportion of mitochondrial oxygen consumption is uncoupled from ATP synthesis under conditions in which adaptational thermogenesis is triggered, i.e. cold exposure in rodents [3]. The heat-generating/futile cycling of the BAT mitochondrial proton

circuit was found to be associated with a specific protein, termed uncoupling protein (UCP, subsequently named UCP1) [3,4]. Despite confinement of UCP1 to BAT under most conditions, significant proton leak occurs in all tissues in which it has been measured [5], leading to the possibility that UCPs are present throughout the body and impact whole-animal metabolic rate. To date, four putative UCP homologues have been identified, with homologue-specific tissue-expression patterns [6].

Mounting evidence indicates that, under appropriate conditions, currently established UCP homologues display uncoupling behaviour (see [6] and references therein). For instance, ectopic expression of putative UCP homologues in mammalian cell lines and yeast leads to a drop in mitochondrial membrane potential ( $\Delta\psi_m$ ), consistent with uncoupling under these conditions. Furthermore, ectopic UCP2 and UCP3 lead to increased  $O_2$  consumption of transformed yeast, as well as elevated heat production *in vitro* in the case of UCP2. In addition, liposome reconstitution experiments using UCP2 and UCP3 indicated that these proteins may catalyse proton flux. Finally, transgenic overexpression of human UCP3 in the skeletal muscle of mice led to enhanced metabolic rate and higher proton leak in isolated mitochondria, with subsequent resistance to body-weight gain and lowered adiposity [7]. Despite such findings, various metabolic parameters (including metabolic rate and body weight) did not differ in UCP3-knockout mice relative to controls [8,9]. In fact, evidence that native UCP3-driven uncoupling primarily influences  $\Delta p$ -sensitive generation of reactive oxygen species [10] is increasingly strong [9]. The latter postulate would be consistent with the dramatic endotoxin-induced rise in mouse skeletal

Abbreviations used: UCP, uncoupling protein; BAT, brown adipose tissue; OGC, 2-oxoglutarate carrier;  $\Delta\psi_m$ , mitochondrial membrane potential;  $\Delta p$ , protonmotive force;  $T_a$ , ambient temperature; OEA, quantitative expression analysis; EST, expressed sequence tag; RT-PCR, reverse transcriptase PCR; GFP, green fluorescent protein; TMRE, tetramethylrhodamine ethyl ester.

<sup>1</sup> To whom correspondence should be addressed (e-mail shadams@gene.com).

muscle UCP3 expression [11], observed concomitant with the development of hypothermia. Thus the molecular basis of cellular thermogenic uncoupling remains to be clarified further, and the potential for as-yet uncharacterized mitochondrial carrier proteins to catalyse uncoupling *in situ* remains a real possibility.

The clear induction of heat-generating pathways in rodent BAT upon exposure to cold ambient temperature ( $T_a$ ) makes this tissue a particularly interesting site for discovery of genes influencing thermogenesis and mitochondrial function. Employing a differential-expression experiment based on this concept, a unique mitochondrial carrier protein, CGI-69, was found to be increased markedly in BAT derived from mice exposed to a cold  $T_a$ . Interestingly, multiple isoforms of human CGI-69 exist with tissue-specific expression, but none were found to influence  $\Delta\psi_m$  when overexpressed in HEK-293 cells. In contrast, overexpression of the human 2-oxoglutarate carrier (OGC), initially designed as a negative control, strongly depressed  $\Delta\psi_m$ . The fact that CGI-69 transfections did not impact  $\Delta\psi_m$  indicates that lowering of  $\Delta\psi_m$  due to mitochondrial damage [12] is not the inevitable result of mitochondrial carrier protein overexpression. Furthermore, the data support the hypothesis that multiple carriers possess uncoupling or other activities which lower  $\Delta\psi_m$ , and raise the intriguing possibility that the OGC participates in physiological proton leak under appropriate conditions.

## EXPERIMENTAL

### Animals and tissue preparation

All studies were done in accordance with guidelines set by the Institutional Animal Care and Use Committee at Genentech (South San Francisco, CA, U.S.A.). Male FVB-N mice (Taconic, Germantown, NY, U.S.A.) were received at 3 weeks of age and housed two per cage until tissue harvest at 6 weeks of age. All mice were fed rodent chow *ad libitum* (Chow 5010, Ralston Purina, St. Louis, MO, U.S.A.) and kept in a 12 h:12 h light/dark cycle (lights on 06:00 h). Control and cold-challenged mice were housed at 22 °C during this 3 week period, whereas warm-acclimated mice were housed at 33 °C, within their thermoneutral zone. For cold-challenged mice, cages were transferred to a 4 °C room for 48 h prior to tissue harvest. Following CO<sub>2</sub>-induced euthanasia in the afternoon, interscapular BAT was excised, cleared carefully of visible white adipose tissue, connective tissue and blood vessels, and snap-frozen in liquid nitrogen for subsequent RNA preparation. For all treatment groups (control, cold-challenged and warm-acclimated), three independent BAT samples were generated for analysis; each sample was composed of BAT pooled from 10 mice.

### Analysis of differentially expressed BAT genes

Samples from each treatment group were transferred to CuraGen Corp. (New Haven, CT, U.S.A.), and RNA was prepared and reverse-transcribed, and subjected to quantitative expression analysis (QEA), the details of which are presented elsewhere [13]. Analyses focused on identification of genes regulated at least 2-fold by changes in  $T_a$ .

### Expression constructs and database searches

Full-length cDNAs of human CGI-69 were generated by PCR, using primers (forward, 5'-CTGAAGCTTCAAGATGGCTG-ACCAG-3', and reverse, 5'-GTCCTTGCCCTCCTTGCCCTTTCAG-3') based on the sequence deposited in a public database (GenBank accession no. AF151827) and using human liver

cDNA as a template (Clontech, Palo Alto, CA, U.S.A.). For subcellular localization studies, a C-terminus FLAG-tagged version (FLAG-huCGI-69) was generated by PCR using the forward primer and a FLAG-reverse primer (5'-CTTGTCATCGTCGTCCTTGTAGTCGCCGCCAGAAAGCCGGTC-3'). CGI-69 PCR products were subcloned from pCR2.1 (Invitrogen, Carlsbad, CA, U.S.A.) into pRK7 (Genentech) for expression analyses. A full-length human OGC cDNA cloned in pINCY (clone 2581467; pINCY-huOGC) was purchased from InCyt Pharmaceuticals (Palo Alto, CA, U.S.A.), and subcloned into pRK5E for expression analyses (pRK5E-huOGC). Compared with the published sequence [14] (GenBank accession no. NM\_003562), pRK5E-huOGC displays a difference (G → A) at position 36 (relative to the start codon ATG) encoding a protein with a single amino acid difference (M12 → I). However, pRK5E-huOGC matches clone 24408 in the public database (GenBank accession no. AF070548). Furthermore, pRK5E-huOGC encodes the most abundant form of OGC in humans, as perusal of the InCyt and public expressed sequence tag (EST) databases indicate that the pRK5E-huOGC protein sequence matches corresponding regions of ESTs derived from at least 22 separate human cDNA libraries (whereas the published sequence did not match any EST at amino acid position 12). Construction of the pcDNA3-UCP3 expression vector is described elsewhere [15].

### Tissue distribution and mRNA analysis

mRNA abundance was analysed in total RNA samples treated with DNase as per the manufacturer's instructions (Gibco-BRL, Grand Island, NY, U.S.A.). Real-time quantitative reverse transcriptase PCR (RT-PCR) was employed as described previously [11,16], using species- and isoform-specific primers and probes recognizing CGI-69. The isoform specificities of the human primer/probe sets were tested against authentic plasmids containing said isoforms. The sequences of primers and probes (5' → 3') are as follows. Human CGI-69 (all isoforms), forward, CCACCTGGTTTCAAGACCCTAC; probe, CGCTTCACTGCGACCATGGATGC; reverse, TGCCTCAGCATCTTCACGAA. Human CGI-69<sub>L</sub>, forward, AGCGAGCTGATGCCTTCCT; probe, CAGACTGTGGAGCTTCTCTATACCAAATTGCC; reverse, CCCTGTGGATTGGAGAGAGG. Mouse CGI-69, forward, CTGGCTCCTGCTTCGCA; probe, TCCGGGCTGAATCTGGCACCA; reverse, GGAAGCCTGCAAAGAGTCCC.

All data were normalized using 18 S mRNA abundance to account for loading differences, using commercially available 18 S primer/probe sets (PE Applied Biosystems, Foster City, CA, U.S.A.).

### $\Delta\psi_m$ measurements and subcellular localization of human CGI-69

Transfections and measurements of  $\Delta\psi_m$  were carried out using protocols described previously [16]. Briefly, HEK-293 cells were co-transfected with pGreen Lantern-1 (green fluorescent protein, GFP; Gibco-BRL) along with pRK7 vector alone (control) or expression vectors containing human CGI-69, OGC or UCP3 (see above). Approx. 24 h later, treatment-related differences in  $\Delta\psi_m$  were determined in GFP-positive cells by monitoring changes in the fluorescence intensity of the  $\Delta\psi_m$ -sensitive dye TMRE (tetramethylrhodamine ethyl ester; Molecular Probes, Eugene, OR, U.S.A.). Just prior to FACS analysis, harvested cells were resuspended in 1 ml of culture medium containing 0.3  $\mu$ M TMRE, and incubated for 30 min at 37 °C in the dark. Cells were washed in culture medium, and then resuspended in 1 ml of culture medium for FACS analysis. The degree of diminution of the  $\Delta\psi_m$  was assessed by the shift in the relative

number of cells displaying lowered  $\Delta\psi_m$ . The transfection protocols employed herein resulted in at least a 30-fold overexpression of each gene as judged by real-time RT-PCR analysis of mRNA abundance in the respective cell populations (results not shown).

For subcellular localization, MCF7 cells were transfected with pcDNA3-FLAG-UCP3 or pRK7-FLAG-huCGI-69, and fixed in 3% formaldehyde as described previously [15]. Incubations with anti-FLAG and anti-cytochrome *c* oxidase antibodies, Cy3- and FITC-conjugated secondary antibodies, and visualization via confocal microscopy were performed as detailed elsewhere [15].

## RESULTS AND DISCUSSION

### Identification and characterization of CGI-69 as a gene induced by cold in BAT

Analysis of BAT genes up-regulated by cold identified a 348 bp gene fragment whose QEA profile indicated significant induction in cold-challenged mice (Figure 1A). Initial identification of this DNA as corresponding to murine EST AA985996 was confirmed by sequencing. Real-time RT-PCR using primers/probes specific to this sequence validated the marked 2-fold cold-induction of the gene in the BAT of cold-challenged mice (Figure 1B). Using murine EST AA985996 as the template for a contig analysis, and using mouse ESTs from the public database (SeqExtend Program, Genentech), a putative murine full-length gene encoding a protein with high similarity to the putative human protein CGI-69 (86% identical/98% similar) was discovered, thus confirming its identity as the mouse orthologue (Figure 2). Interestingly, analysis of the CGI-69 protein structure indicated the presence of four mitochondrial carrier domains (see the Figure 2 legend), six potential transmembrane-spanning regions, a likely mitochondrial localization (NNPSL algorithm; Sanger Centre, Hinxton, Cambs, U.K.) and three regions with reasonable homologies to putative mitochondrial energy-transfer signature motifs present in known UCP functional family members (Figure 2).

The significant cold-induction of BAT CGI-69 expression (Figure 1), putative mitochondrial localization of the protein, and the presence of mitochondrial carrier motifs raised the possibility that this previously uncharacterized protein represents a new member of the UCP functional family. However, alignment of CGI-69 with known sequences of UCP homologues, the citrate carrier, OGC and ADP/ATP translocases, indicated an equivalent similarity (approx. 20%) to each (results not shown), with a likelihood of significant evolutionary distance between CGI-69 and the UCPs based on an alignment tree analysis (Figure 2, bottom panel). The lack of experimental data regarding the biology of CGI-69 prompted us to obtain the full-length clone of human CGI-69 for clarification of this protein's potential for uncoupling behaviour *in vitro*.

### Presence of human CGI-69 variants and lack of effect of CGI-69 overexpression on $\Delta\psi_m$

A variety of CGI-69 clones were isolated from human liver upon PCR amplification and cloning (see the Experimental section), one of which corresponded to the original AF151827 sequence in GenBank ('CGI-69', Figure 2). Numerous clones derived from separate independent PCR cloning efforts diverged from the GenBank sequence in that they encoded an eight-amino-acid insert preceded by a W64 → L amino acid difference, plus an F247 → L change (Figure 2): this 'long version' isoform was termed CGI-69<sub>L</sub> (CGI-69<sub>L</sub> GenBank accession no. AF317711). In addition, various clones not depicted in Figure 2 encoded

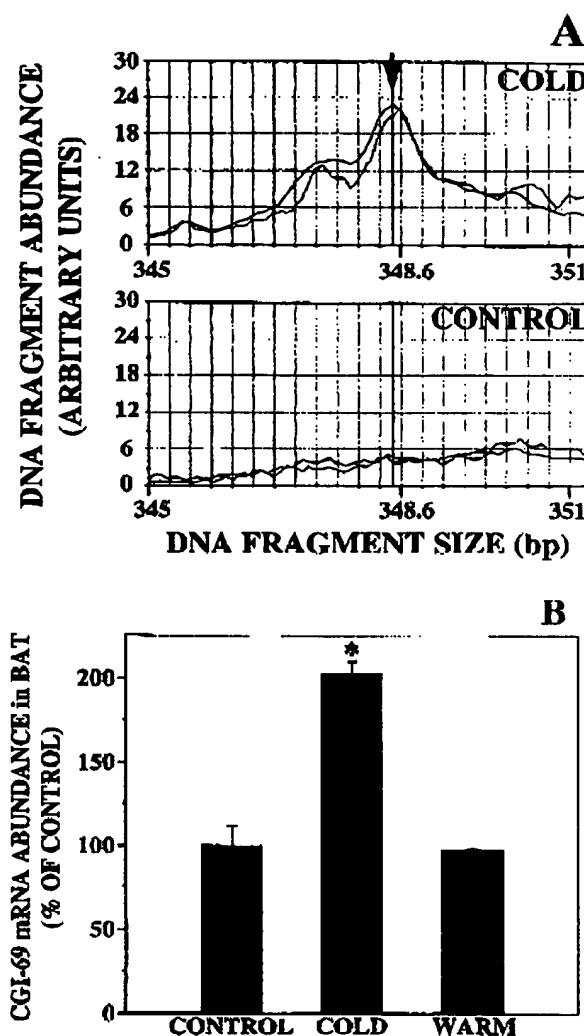
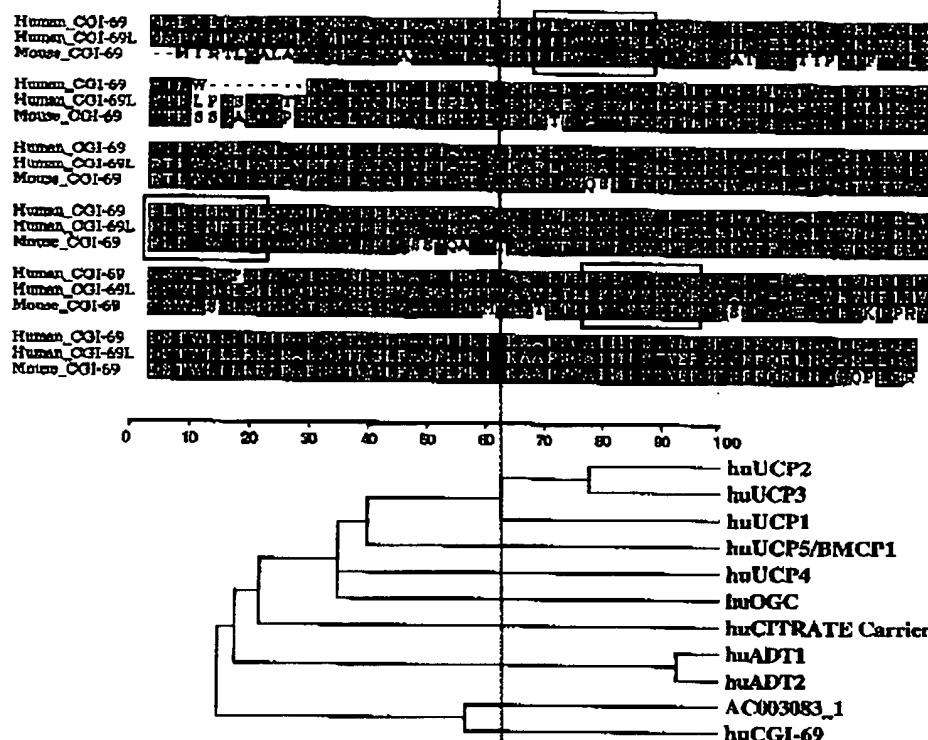


Figure 1 Murine CGI-69 gene expression in BAT is triggered by cold exposure

mRNA was obtained from the BAT of 6-week-old male FVB-N mice raised at 22 °C postweaning (controls), at thermoneutrality (33 °C, warm-acclimated) or at 22 °C but challenged with 48 h exposure to 4 °C (cold-challenged). (A) Example of QEA of a BAT mRNA transcript modified by temperature (see the Experimental section). The peak height corresponds to CGI-69 cDNA fragment abundance, which in turn corresponds to CGI-69 mRNA transcript in the original sample (two samples/temperature shown). The arrow denotes the gel location (348 bp) of the fragment peak. Warm-acclimated mouse samples (results not shown) gave a similar profile to controls. (B) Induction of CGI-69 expression by cold exposure was confirmed through real-time RT-PCR quantification of mouse BAT mRNA ( $n = 3/\text{group}$ ). Cold caused a 2 fold rise in transcript abundance ( $P < 0.01$ , Student's *t* test) in cold-challenged mice versus controls. Error bars represent S.E.M.

a protein matching the GenBank sequence but containing the F → L change (F239 → L in CGI-69). CGI-69 transcript was detected in numerous tissues, with particularly strong abundance in testis and BAT of mice, and testis and kidney of humans (Figure 3). In humans, both the short form(s) and long form(s) of the gene were expressed at various ratios (see the Figure 3 legend).



**Figure 2** The amino acid sequence of human CGI-69 reveals mitochondrial carrier protein domains and the presence of variant isoforms

Cloning efforts uncovered at least two isoforms of human CGI-69 (CGI-69 and CGI-69L). The putative full-length mouse protein derived from contig analysis, showing high similarity to the human protein, is also shown for comparison. Boxes correspond to regions of mitochondrial energy-transfer signature motifs found in UCPs and which are reasonably well preserved in CGI-69. Mitochondrial carrier domains (Pfam) in human CGI-69 correspond to residues 10–48, 97–144, 152–276 and 298–340. (Bottom panel) Alignment tree of human mitochondrial carriers indicating likely evolutionary distance between CGI-69 and the UCPs. AC003083 is a putative human protein deposited in GenBank which shows similarity to CGI-69 (51% identity/68% similarity). ADT, ADP/ATP translocase; BMCP1, brain mitochondrial carrier protein-1.

An initial assessment of possible uncoupling activity of candidate proteins may be made through the use of  $\Delta\psi_m$ -sensitive dyes such as TMRE, whose fluorescence intensity in cell preparations diminishes in response to lowered  $\Delta\psi_m$ . To date, such an approach has successfully characterized UCPs in mammalian cell lines and yeast [15, 17–20], with the caveat that  $\Delta\psi_m$  is also influenced by additional pathways (electron transfer, ATP turnover) that generate or dissipate  $\Delta\psi_m$ .

As shown in Figure 4, overexpression of human CGI-69 in HEK-293 cells did not influence  $\Delta\psi_m$ , in marked contrast with the significant diminution observed after overexpression of human UCP3. Equivalent results were obtained with overexpression of CGI-69<sub>L</sub> and the F239L variant of CGI-69 (results not shown). Importantly, the mitochondrial localization of C-terminally FLAG-tagged CGI-69 (Figure 5) indicates that native CGI-69 is targeted to this organelle. It has been proposed that damage to mitochondria from overexpression of mitochondrial carrier proteins could explain uncoupling characteristics of said carriers [12]. This scenario did not appear to hold true in the case of CGI-69, as no evidence for uncoupling emerged despite significant overexpression and mitochondrial localization.

Notably, it was found that overexpression of C-terminally FLAG-tagged CGI-69 in HEK-293 cells diminished  $\Delta\psi_m$  to a similar magnitude as UCP3 (results not shown), an unanticipated result based on the lack of effect of untagged CGI-69 on  $\Delta\psi_m$  (Figure 4). Such findings may simply reflect an interesting change

in biochemical activity for CGI-69 when certain artificial manipulations are made to the C-terminus of the protein. Nevertheless, the possibility emerged that untagged CGI-69 lacked a  $\Delta\psi_m$ -lowering effect due to poor mitochondrial localization compared with the C-terminally FLAG-tagged protein. While unlikely, this scenario was tested through overexpression of N-terminally FLAG-tagged CGI-69 in HEK-293 cells. As for untagged CGI-69, N-terminally FLAG-tagged CGI-69 had no effect on  $\Delta\psi_m$ , despite mitochondrial localization in MCF7 cells (results not shown). These results further support the suggestion that native CGI-69 does not lower  $\Delta\psi_m$ , and indicate that studies involving manipulation of the C-terminus of CGI-69 can lend insight into mechanisms by which mitochondrial carriers impact on  $\Delta\psi_m$ . For example, it is possible that introduction of the negatively charged C-terminal FLAG-tag (DYKDDDDK) elicits an alteration in the protein's affinity for certain ions, thus changing its activity. Furthermore, CGI-69 might interact with regulatory proteins in the cell; alteration of the C-terminus could abolish or enhance such interactions, leading to functional changes.

#### Human OGC lowers $\Delta\psi_m$ in vitro

The current experimental strategy employed the human OGC as a negative control. This approach was logical based on the electroneutral nature of 2-oxoglutarate<sup>2-</sup>/malate<sup>2-</sup> exchange

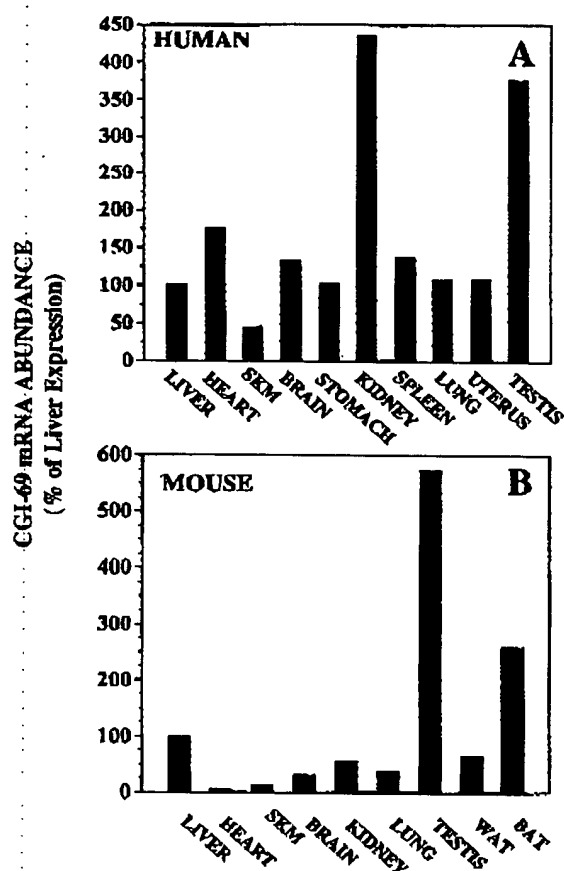


**Figure 3** Tissue-specific expression of CGI-69 in humans and mice

Transcripts for CGI-69 were widely detected in (A) human and (B) mouse tissues, with particularly high expression in testis (both species), kidney (human) and BAT (mouse). All values are expressed relative to liver CGI-69 mRNA abundance, and represent abundance of total CGI-69. The relative contribution of CGI-69 (percentage of total CGI-69 transcript) in humans was: 23% (skeletal muscle, SKM),  $\approx$  40–45% (heart, stomach, lung, uterus), 59% (brain),  $\approx$  72% (liver, spleen), 80% (kidney) and 91% (testis). Human RNA samples were purchased from Clontech. WAT, white adipose tissue.

catalysed by the carrier [21], its clear localization to the mitochondrial inner membrane [22] and its reported lack of effect on mitochondrial function in OGC-transformed yeast, including  $\Delta\psi_m$  [20].

To our surprise, overexpression of the human OGC significantly diminished  $\Delta\psi_m$  (Figure 4), possibly signalling a previously unappreciated uncoupling activity of this protein. Indeed, OGC was almost as powerful as UCP3 in eliciting a drop in  $\Delta\psi_m$  of HEK-293 cells, as judged by the number of cells displaying lowered  $\Delta\psi_m$  (Figure 4B). (In preliminary experiments using a Clark-type  $O_2$  electrode (see [11] for details),  $O_2$  consumption in populations of HEK-293 cells transiently transfected with the human OGC and assayed in high-glucose Dulbecco's modified Eagle's medium was 28% higher (at 2.0 nmol of  $O_2$ /min per  $10^6$  cells) than controls in the presence of 1  $\mu$ g/ml oligomycin. Similarly, oligomycin-insensitive  $O_2$  consumption was 74% higher in UCP3-transfected cells (2.8 nmol of  $O_2$ /min per  $10^6$  cells) compared with controls. Higher  $O_2$  consumption occurred

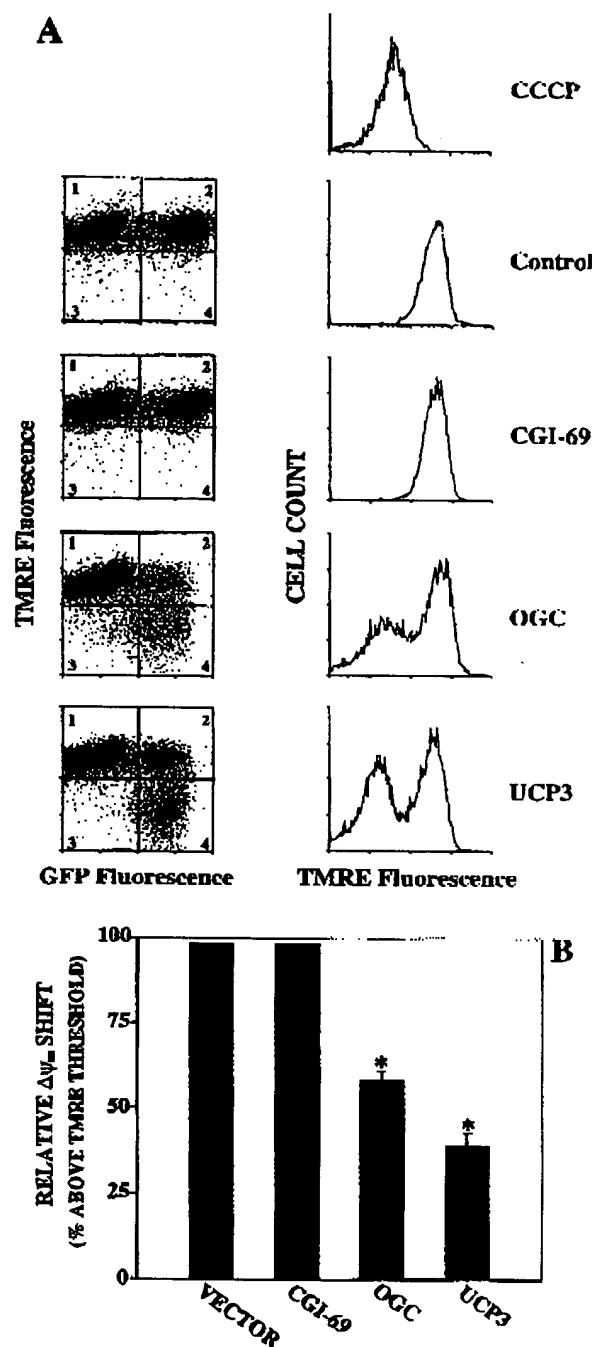


**Figure 4** Overexpression of the human OGC depolarizes mitochondria of HEK-293 cells, whereas CGI-69 is without effect

(A) FACS analysis data from cells transfected with GFP plus vector alone (controls) or constructs containing the human mitochondrial carriers CGI-69, OGC or UCP3 (positive control). The right-hand panels depict the TMRE-fluorescence intensity profiles of GFP-positive cells (windows 2 and 4 of the left-hand panels), with a leftward shift relative to controls indicative of cells displaying a lowered  $\Delta\psi_m$ . Also shown are data from cells treated with the chemical uncoupler CCCP (carbonyl cyanide *m*-chlorophenylhydrazone, 50  $\mu$ M). (B) Diminished  $\Delta\psi_m$  in OGC- or UCP3-transfected cells was significant, as judged by a drop in the relative number of GFP-positive cells displaying TMRE fluorescence intensity equal to that of controls (percentage of cells remaining in windows 2 in the left-hand panels of A). \* $P < 0.01$  compared with controls;  $n = 8$ /treatment, Student's *t* test.

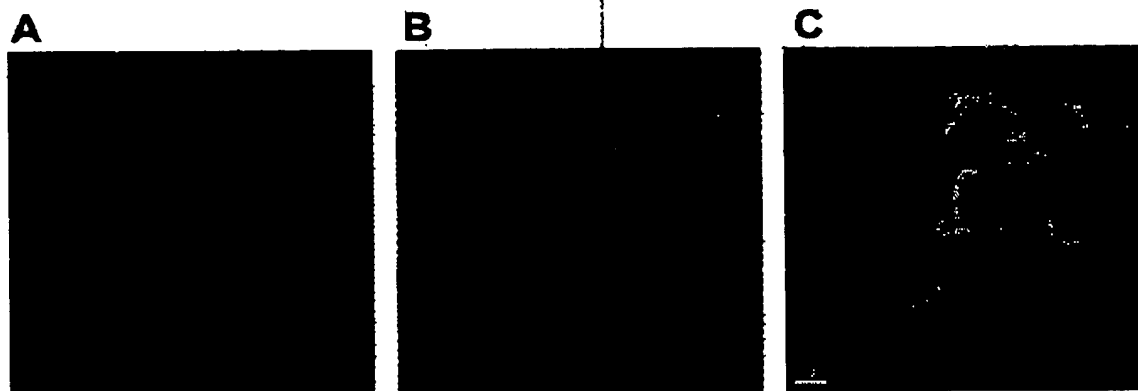


**Figure 5** Human FLAG-tagged CGI-69 is localized to the mitochondria of MCF7 cells

Employing anti-cytochrome *c* oxidase and anti-FLAG antibodies, the subcellular localization of FLAG-tagged CGI-69 was determined by confocal microscopy (see the Experimental section). Mitochondrial cytochrome *c* oxidase (A, green staining) co-localized with C-terminally FLAG-tagged CGI-69 (B, red staining), as evidenced by the yellow colour upon superimposing the images (C). Not shown are similar results obtained with FLAG-tagged UCP3 and N-terminally FLAG-tagged CGI-69.

despite a dilution effect from untransfected cells (transfection efficiencies approx. 30–40%), and despite the presence of a persistently lowered  $\Delta\psi_m$  in OGC- or UCP3-transfected cells (cells displaying a leftward TMRE fluorescence shift, as in Figure 4) treated with oligomycin (results not shown). Oxygen consumption values in the absence of oligomycin were 2.9 (controls), 3.1 (OGC) and 3.5 nmol of O/min per  $10^6$  cells (UCP3). Based on such results, one may not exclude the possibility that the OGC (and perhaps other carriers not currently thought to have uncoupling activity) could influence global proton leak in mammals. Further extensive studies would be required to ascertain whether the diminution of  $\Delta\psi_m$  represents a truly physiological phenomenon, or results from changes in the folding or insertion of the OGC in mitochondria following artificial over-expression.

It is intriguing to consider that an OGC-driven drop in  $\Delta\psi_m$  may be due in part to 'indirect' uncoupling via stimulation of flux through the malate/aspartate shuttle: electrogenic co-transport of a proton plus glutamate<sup>-</sup> into the mitochondrion occurs in exchange for aspartate<sup>-</sup> in the course of this shuttle's operation [21]. However, the quantitative contribution of such a pathway, which transports only a single proton per cycle, towards establishment of the marked drop in  $\Delta\psi_m$  caused by the OGC overexpression will require further detailed evaluation (i.e. using inhibitors of the shuttle such as amino-oxyacetate or phenylsuccinate). Unlike the current study, ectopic expression of the OGC in yeast reportedly failed to alter  $\Delta\psi_m$  or other metabolic parameters [20]. Therefore, it would be interesting to test whether the yeast strain employed in that study possesses an operational glutamate/aspartate carrier and an active malate/aspartate shuttle. Based on currently available information, the existence of such systems in yeast has not been established firmly (F. Palmieri, personal communication). Alternatively, the OGC may catalyse a different mechanism of proton/ion transport, or influence other pathways which generate or dissipate  $\Delta\psi_m$  in mammalian cells. Experiments designed to measure  $\Delta\psi_m$  and oxygen consumption upon titration of  $\Delta\psi_m$ -generating and -dissipating systems, preferably in stable cell lines overexpressing the

OGC, should pinpoint the mechanism by which the OGC impacts on  $\Delta\psi_m$ .

#### Summary and conclusions

The data suggest that the unique carrier CGI-69 does not possess uncoupling behaviour, but rather serves a different physiological role in mitochondria. Significant induction of BAT CGI-69 transcript in cold-challenged mice (Figure 1) could signal activity which supports the enhanced ion and metabolite flux inherent to thermogenic BAT. Strong expression in the testes of CGI-69 in mice and humans (Figure 3) may point to involvement of the protein in modulation of mitochondrial function in this tissue. Finally, the biochemical potential of the OGC to lower  $\Delta\psi_m$  in HEK-293 cells is a novel finding, and is suggestive of uncoupling behaviour under these experimental conditions. Such assertions require more rigorous testing, through examinations of mitochondrial carrier activities *in vitro* and in the context of the whole animal.

We thank Wenlu Li for confocal microscopy assistance, and the Genomics Facility at CuraGen for valuable technical support. Anti-cytochrome *c* oxidase was a gift from G.-A. Keller.

#### REFERENCES

- Brand, M. D., Chien, L.-F., Ainscow, E. K., Rolfe, D. F. S. and Porter, R. K. (1994) The causes and functions of mitochondrial proton leak. *Biochim. Biophys. Acta* **1187**, 132–139.
- Rolfe, D. F. S., Newman, J. M. B., Buckingham, J. A., Clark, M. G. and Brand, M. D. (1999) Contribution of mitochondrial proton leak to respiration rate in working skeletal muscle and liver and to SMR. *Am. J. Physiol.* **276**, C692–C699.
- Nicholls, D. G. and Locke, R. M. (1984) Thermogenic mechanisms in brown fat. *Physiol. Rev.* **64**, 1–64.
- Ricquier, D., Castella, L. and Bouillaud, F. (1991) Molecular studies of the uncoupling protein. *FASEB J.* **5**, 2237–2242.
- Rolfe, D. F. S., Hulbert, A. J. and Brand, M. D. (1994) Characteristics of mitochondrial proton leak and control of oxidative phosphorylation in the major oxygen-consuming tissues of the rat. *Biochim. Biophys. Acta* **1118**, 405–416.

- 6 Adams, S. H. (2000) Uncoupling protein homologs: emerging views of physiological function. *J. Nutr.* **130**, 711–714.
- 7 Clapham, J. C., Arch, J. R. S., Chapman, H., Haynes, A., Lister, C., Moore, G. B. T., Piercy, V., Carter, S. A., Lehner, I., Smith, S. A. et al. (2000) Mice overexpressing human uncoupling protein-3 in skeletal muscle are hyperphagic and lean. *Nature (London)* **406**, 415–418.
- 8 Gong, D.-W., Monemdjou, S., Gavrilova, D., Leon, L. R., Marcus-Samuels, B., Chou, C. J., Everett, C., Kozak, L. P., Li, C., Deng, C., Harper, M.-E. and Reitman, M. L. (2000) Lack of obesity and normal response to fasting and thyroid hormone in mice lacking uncoupling protein-3. *J. Biol. Chem.* **275**, 16251–16257.
- 9 Vidal-Puig, A. J., Grujic, D., Zhang, C.-Y., Hagen, Y., Boss, O., Ido, Y., Szczepanik, A., Wade, J., Mootha, V., Cortright, R., Muoio, D. M. and Lowell, B. B. (2000) Energy metabolism in uncoupling protein 3 gene knockout mice. *J. Biol. Chem.* **275**, 16258–16266.
- 10 Skulachev, V. P. (1998) Role of uncoupled and non-coupled oxidations in maintenance of safely low levels of oxygen and its one-electron reductants. *D. Rev. Biophys.* **29**, 169–202.
- 11 Yu, X. X., Barger, J. L., Boyer, B. B., Brand, M. D., Pan, G. and Adams, S. H. (2000) Impact of endotoxin on UCP homolog mRNA abundance, thermoregulation, and mitochondrial proton leak kinetics. *Am. J. Physiol. Endocrinol. Metab.* **279**, E433–E446.
- 12 Brand, M. D., Brindle, K. M., Buckingham, J. A., Harper, J. A., Rolfe, D. F. S. and Stuart, J. A. (1999) The significance and mechanism of mitochondrial proton conductance. *Int. J. Obesity* **23** (suppl. 6), S4–S11.
- 13 Shinkets, R. A., Lowe, D. G., Tai, J. T., Sehl, P., Jiri, H., Yang, R., Predki, P. F., Rothberg, B. E., Murtha, M. T., Roth, M. E. et al. (1999) Gene expression analysis by transcript profiling coupled to a gene database query. *Nat. Biotechnol.* **17**, 798–803.
- 14 Iacobazzi, V., Palmieri, F., Runswick, M. J. and Walker, J. E. (1992) Sequences of the human and bovine genes for the mitochondrial 2-oxoglutarate carrier. *DNA Sequence* **3**, 79–88.
- 15 Mao, W., Yu, X. X., Zhong, A., Li, W., Brush, J., Sherwood, S. W., Adams, S. H. and Pan, G. (1999) UCP4, a novel brain-specific mitochondrial protein that reduces membrane potential in mammalian cells. *FEBS Lett.* **443**, 326–330.
- 16 Yu, X. X., Mao, W., Zhong, A., Schow, P., Brush, J., Sherwood, S. W., Adams, S. H. and Pan, G. (2000) Characterization of novel UCP5/BMCP1 isoforms, and differential regulation of UCP4 and UCP5 expression through dietary or temperature manipulation. *FASEB J.* **14**, 1611–1618.
- 17 Fleury, C., Neveleva, M., Collins, S., Raimbault, S., Champigny, O., Lévi-Mayrueis, C., Bouitaud, F., Seldin, M. F., Surwit, R. S., Ricquier, D. and Warden, C. H. (1997) Uncoupling protein-2: a novel gene linked to obesity and hyperinsulinemia. *Nat. Genet.* **15**, 269–272.
- 18 Gimeno, R. E., Demski, M., Wang, X., Deng, N., Shyjan, A. W., Gimeno, C. J., Iris, F., Ellis, S. J., Woolf, E. A. and Tartaglia, L. A. (1997) Cloning and characterization of an uncoupling protein homolog. A potential molecular mediator of human thermogenesis. *Diabetes* **46**, 900–906.
- 19 Gong, D.-W., He, Y., Karas, M. and Reitman, M. (1997) Uncoupling protein-3 is a mediator of thermogenesis regulated by thyroid hormone,  $\beta$ -adrenergic agents, and leptin. *J. Biol. Chem.* **272**, 24129–24132.
- 20 Sanchez, D., Fleury, C., Chomiki, N., Gouborn, M., Huang, Q., Neveleva, M., Crégoire, F., Eastlick, J., Raimbault, S., Lévi-Mayrueis, C. et al. (1998) BMCP1, a novel mitochondrial carrier with high expression in the central nervous system of humans and rodents, and respiration uncoupling activity in recombinant yeast. *J. Biol. Chem.* **273**, 34611–34615.
- 21 LaNoue, K. and Schoolwerth, A. C. (1979) Metabolite transport in mitochondria. *Annu. Rev. Biochem.* **48**, 671–692.
- 22 Palmisano, A., Zara, V., Hönlinger, A., Voza, A., Dekker, P. J. T., Pfanner, N. and Palmieri, F. (1998) Targeting and assembly of the oxoglutarate carrier: general principles for biogenesis of carrier proteins of the mitochondrial inner membrane. *Biochem. J.* **333**, 151–158.

Received 2 July 2000/3 October 2000; accepted 7 November 2000